Higher order color mechanisms: Evidence from noise-masking experiments in cone contrast space

Thorsten Hansen

Department of Psychology,
Justus Liebig University Gießen, Gießen, Germany

Karl R. Gegenfurtner

Department of Psychology,
Justus Liebig University Gießen, Gießen, Germany

This study addresses a fundamental question concerning the number of cortical, i.e., higher order mechanisms in color vision. The initial subcortical stages in color vision can be described by three cone mechanisms, S, M, L, and three pairs of second-stage mechanisms (achromatic $L + M$ and $-L - M$, chromatic $S - (L + M)$ and $-S + (L + M)$, and chromatic $L - M$ and $M - L$). The further mechanistic description of cortical color vision is controversial. On the one hand, numerous studies that defined their stimuli in a color-opponent Derrington-Krauskopf-Lennie (DKL) color space found evidence for higher order mechanisms. On the other hand, some studies that defined their stimuli in cone contrast (CC) space failed to find such evidence. Here we show that this failure was due to a restricted choice of stimuli. We used a noise-masking paradigm to measure discrimination thresholds for textured patterns modulated along chromatic directions in CC space. Unlike previous studies we defined noise directions in DKL space and converted them to CC space. When the noise contrast was sufficiently high we found selective masking, but this did not occur when the noise contrast was low. Selective masking indicates higher order mechanisms, since so far no alternative model has been proposed. Previous studies in CC space failed to find selective masking due to the low contrast of the noise and due to the restricted choice of perceptually highly similar noise directions that mainly stimulated the second-stage mechanisms. We conclude that cortical color vision is governed by higher order mechanisms.

Keywords: color vision, higher order color mechanisms, noise masking

Introduction

Color (including achromatic light modulations) is processed along a hierarchy of different stages. The first subcortical stages are the cone photoreceptors in the retina, the retinal ganglion cells (RGCs), and neurons in the lateral geniculate nucleus (LGN). At the first stage, three types of cone photoreceptors, S, M, and L, respond to light, i.e., to a spectrum of electromagnetic radiation between approximately 400 and 700 nm (Stockman & Sharpe, 1999). The three types of cones have broad-band and overlapping absorption spectra such that the cone responses are highly correlated. Each type of cone can be abstracted as a *mechanism* that transforms a high-dimensional light spectrum into a single number, the cone response.

The idea of the mechanistic approach is to model color vision as a series of processing stages and characterize the transformation at each stage by a transformation of the cone mechanisms into a new set of second-order, third-order, and so forth mechanisms (Stockman & Brainard, 2009). A mechanism can be characterized by a weighted combination of cone signals (Eskew, 2008, 2009). Mechanisms are univariant and convey just a single nonnegative scalar quantity (Watson & Robson, 1981; Graham, 1989).

At the second stage, the cone responses are processed by a network of retinal neurons whose output is conveyed by RGCs that project to the LGN. RGC responses are decorrelated compared to the responses of the three types of cones (Buchsbaum & Gottschalk, 1983). The transformation within this network can be abstracted as the combination of the three cone mechanisms into three second-stage, postreceptoral mechanisms: an achromatic $L + M$ mechanism and two chromatic mechanisms, $S - (L + M)$ and $L - M$. More precisely, each second-stage mechanism has a negative counterpart $-L - M$, $-S + (L + M)$, and $M - L$. (A summary of all notations is given in Appendix A.) This coding can represent contrast increments and decrements relative to a background by unipolar mechanisms that convey only a single, nonnegative scalar quantity. The properties of RGCs and their LGN target neurons are highly similar (Dacey, 2000). The chromatic mechanisms in the LGN of macaque

correspond to the two cardinal chromatic mechanisms of RGCs (Derrington, Krauskopf, & Lennie, 1984).

To sum up, mechanisms are conventionally used to characterize the initial stages of color vision. The first stage is governed by three cone mechanisms, S, L, and M, that are combined at the second stage into six second-stage mechanisms, a pair of achromatic mechanisms, $L + M$ and $-L - M$, and two pairs of chromatic mechanisms, $S - (L + M)$ and $-S + (L + M)$ and $L - M$ and $M - L$.

While the subcortical stages of color vision in the cones and in RGCs and LGN neurons can be mechanistically characterized reasonably well, the further mechanistic description of cortical color vision is controversial. In particular, no consensus has been reached about the number and nature (e.g., the tuning width) of cortical mechanisms. One reason is that mechanisms cannot be directly accessed in psychophysical experiments but have to be inferred from measured data based on the intrinsic features of *models* that can account for these data. For example, in noise-masking experiments, masking curves can be measured, but these curves are in general different from the tuning curve of the underlying mechanisms (D'Zmura & Knoblauch, 1998). We use the term "noise-masking curve" to denote experimentally measured curves and the term "tuning curves" to denote the inferred response curves of the underlying mechanisms to stress this difference. The problem with the indirect model approach is that a hypothesis can only be substantiated but not falsified. For example, even if dozens of models with second-stage mechanisms fail to account for a given data set, there may be still a particular sophisticated second-stage model that may account for this data set.

Another reason for the controversy about higher order mechanisms may be that different experiments may have tapped into different chromatic processing stages differing in the number and nature of their underlying mechanisms. From physiological experiments we know that the relative number of nonlinear neurons with a sharp chromatic tuning increases along the visual pathway (for a review, see, e.g., Gegenfurtner, 2003). Further, the mechanistic psychophysical approach may be inappropriate to characterize the complex nonlinear recurrent interactions at adaptable, plastic higher cortical processing stages, and, last but not least, there is no precise definition of what constitutes a "mechanism" that is common to all experiments and experimenters (Stockman & Brainard, 2009).

Numerous psychophysical experiments have found evidence for higher order color mechanisms, using adaptation (Krauskopf, Williams, Mandler, & Brown, 1986; Webster & Mollon, 1991), studying chromatic discrimination (Krauskopf & Gegenfurtner, 1992), or employing noise-masking paradigms (Gegenfurtner &

Kiper, 1992; Li & Lennie, 1997; D'Zmura & Knoblauch, 1998; Stromeyer, Thabet, Chaparro, & Kronauer, 1999; Goda & Fujii, 2001; Lindsey & Brown, 2004; Hansen & Gegenfurtner, 2006; Cass, Clifford, Alais, & Spehar, 2009). Even for the classical study defining the "cardinal directions of color space" (Krauskopf, Williams, & Heeley, 1982), a re-analysis of the original data found evidence for "higher order color mechanisms" (Krauskopf et al., 1986).

All these studies specified their stimuli in a Derrington-Krauskopf-Lennie (DKL) color space. In contrast, in the few studies in which the stimuli were specified in cone contrast (CC) space no evidence for higher order mechanisms was found (Sankeralli & Mullen, 1997; Giulianini & Eskew 1998).

The correlation between the color space used and the findings is not a coincidence. In principle the color space used to specify the stimuli should be irrelevant since all colors can be specified in any color space. However, the particular choice of color space can affect the *sampling of stimulus directions* (Eskew, 2009; Stockman & Brainard, 2009). Consider, for example, a color space 1 where chromatic directions are highly compressed, while others are expanded relative to color space 2, such that some chromatic direction are separated by 90 deg in color space 1 but almost identical in color space 2. Then the selection of hue directions for a particular experiment may be biased by this transformation and may be different depending on the color space. This is exactly the situation for CC and DKL space, where the mapping of angles is highly nonlinear (Figure 1). In particular, all angles in the second and fourth quadrants of the plane spanned by the $\Delta L/L$ and $\Delta M/M$ axes of CC space map to a small area in DKL space around the L/M axis. Modulations along chromatic directions in these quadrants can be up to 90 $\deg_{CC}$ apart in CC space but stimulate almost exclusively a single pair of second-stage mechanisms, namely $L - M$ and $M - L$.

An earlier study has provided some evidence that higher order color mechanisms are approximately equally spaced in DKL space (Hansen & Gegenfurtner, 2006). If the mapping nonlinearity is not taken into account, angles may be chosen in CC space that would activate essentially only second-stage mechanisms. Higher order mechanisms will then be missed due to this sampling bias. For example, Giulianini & Eskew (1998) used noise angles of 90 and 135 $\deg_{CC}$ that differ considerably by 45 deg in CC space. However, the corresponding angles in DKL space (7.1 and 1.6 $\deg_{DKL}$) are just 5.5 $\deg_{DKL}$ apart. Modulations along these directions stimulate almost exclusively a single pair of second-stage mechanisms ($L - M$ and $M - L$) (Figure 2, right). The measured masking curves for both noise directions were quite similar (Figure 2, left, black and green curves) and Giulianini and Eskew
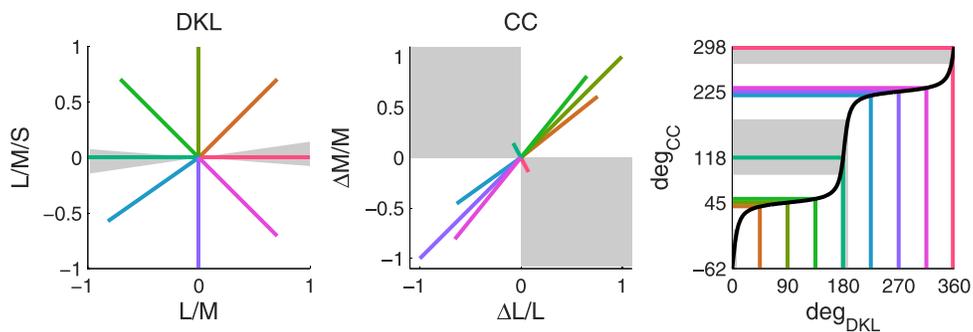
Figure 1. The mapping of equidistant angles from DKL to CC space is highly nonlinear. Chromatic directions in CC space of 0 and 90 deg$_{CC}$ correspond to chromatic directions of 176.1 and 7.1 deg$_{DKL}$ in DKL space. Thus half of the angles in CC space (gray-shaded area, second and fourth quadrant) are mapped to only 3.5% of the angles in DKL space. In contrast, chromatic directions that are separated by 90 deg$_{DKL}$ in DKL space (such as 45–135 deg$_{DKL}$ or 225–315 deg$_{DKL}$) are mapped to almost the same chromatic direction in CC space (45 deg$_{CC}$ or 225 deg$_{CC}$, respectively). When investigating higher order mechanisms these nonlinearities have to be taken into account such that angles in CC space are selected (e.g., 39, 45, and 51 deg$_{CC}$) that differ with respect to the purported mechanisms, instead of those (e.g., 90, 135 deg$_{CC}$) that stimulate almost exclusively a single pair of second-stage mechanisms (L − M and M − L). Lines are pseudocolored for visualization.

(1998) specified a model with second-stage mechanisms that could account for the data.

These previous studies have used noise directions that when mapped to DKL would almost exclusively stimulate a single pair of second-stage mechanisms (L − M and M − L) and therefore could account for their

data by only few second-stage mechanisms (Sankeralli & Mullen, 1997; Giulianini & Eskew, 1998). The limitation of the noise directions chosen has been noted before: Stromeyer et al. (1999, p. 2110), stated that "their [Giulianini & Eskew, 1998] masks were far more effective for the RG [i.e., the L − M and M − L
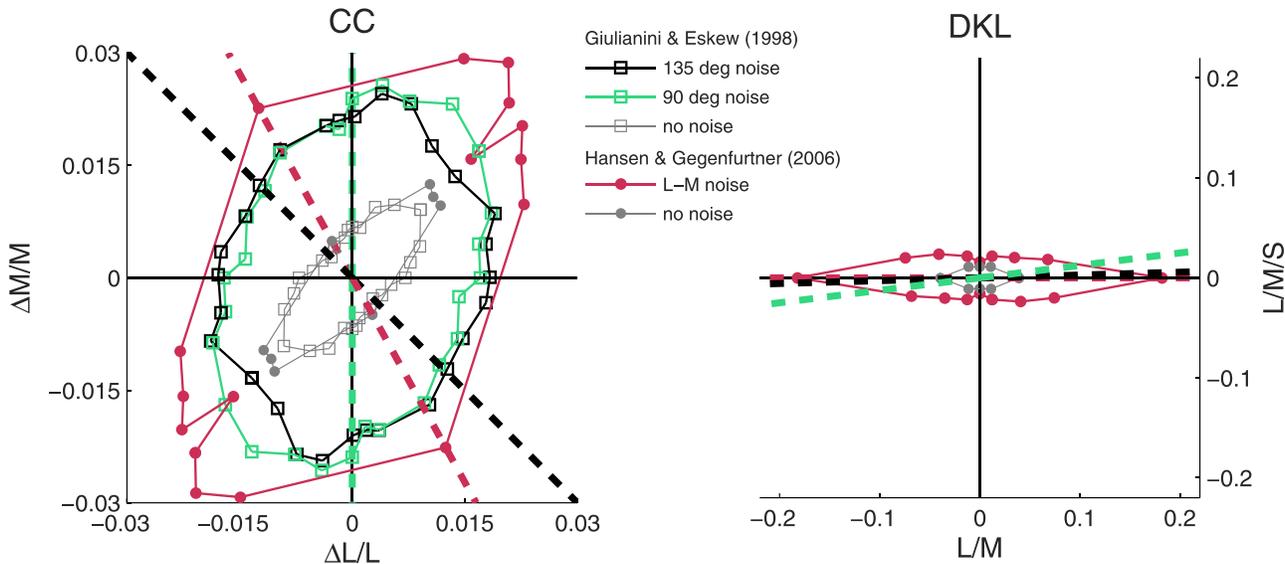

Figure 2. Noise-masking curves for the detection of Gabor patches embedded in chromatic ring-noise of two directions (90 deg$_{CC}$, green dashed line, green open squares; and 135 deg$_{CC}$, black dashed line, black open squares) measured for a single observer (left), redrawn from Figure 5 of Giulianini and Eskew (1998). The noise angles of 90 and 135 deg differ considerably by 45 deg$_{CC}$ in CC space. However, these noise angles map to chromatic directions 7.1 deg$_{DKL}$ and 1.6 deg$_{DKL}$ in DKL space, that are just 5.5 deg apart and stimulate almost exclusively a single pair of second-stage mechanisms (L − M and M − L) (red dashed line) at 0/180 deg$_{DKL}$ in DKL space (right). Consequently, Giulianini and Eskew (1998) measured the same threshold elevations for the two noise directions tested and found no evidence for more than two mechanisms. The threshold contours are also in good agreement with noise-masking curves (red) for noise modulated along the L/M axis of DKL space (red dashed line); data from Figure 6 of Hansen and Gegenfurtner (2006). Data for the no-noise condition measured in both studies are in good agreement (Giulianini & Eskew, open gray squares; Hansen & Gegenfurtner, gray dots).

mechanisms] mechanism, and hence not well balanced in stimulating RG and LUM [i.e., L + M and –L– M]"; and Eskew (2009, p. 2693), stated that "a clear weakness of the studies by Sankeralli & Mullen (1997) and Giulianini & Eskew (1998) was that noise was never placed in the corners of the detection contours." Overall, Giulianini and Eskew (1998) tested if there are mechanisms with equal and opposite CC weights for L and M which are sensitive enough to dominate detection under the conditions of their experiments. Their results were consistent with this hypothesis and helped to characterize these mechanisms. However, their stimuli were unsuitable to address the more general question of the number of chromatic mechanisms in the $\Delta L/\Delta M$ color plane.

The aim of the present study

Our goal was to get to the root of the discrepancy between the different studies. We set out to investigate whether noise directions can be chosen in CC space that result in selective masking. This would resolve one major issue that has arisen over the years, since the seeming lack to find selective masking in CC space has been the major argument against the existence of higher order mechanisms.

To achieve this goal, it has to be assumed that different higher order mechanisms are stimulated. From previous investigations we know the directions in DKL space that stimulate different mechanisms (Hansen & Gegenfurtner, 2006). First, we investigated the highly nonlinear transformation of chromatic directions between CC and DKL space (Figure 1). We then defined our noise directions in DKL space such that they stimulated different chromatic mechanisms when mapped to CC space. Next we used these directions in CC space to run noise-masking experiments with noise of equal contrast in CC space. Because we used stimuli in previous studies that had equal noise power when represented in DKL space, the results of these studies could not be simply transformed to CC space. In the present study we selected our stimuli to have equal noise power when represented in CC space. We found selective masking, but only if the noise contrast was sufficiently high.

We hypothesized that previous studies failed to find selective masking because the stimuli were not optimally selected to distinguish the relevant competing hypotheses. With a more complete choice of stimuli in CC space we found selective masking.

Eskew (2009) has presented overwhelming evidence for selective masking in his extensive review, and here we show that selective masking can also be found if the stimuli are specified in CC space. At present, the only model that can account for selective masking and its dependence on the type of noise comprises multiple broadly tuned mechanisms (Hansen & Gegenfurtner, 2006). We suggest that cortical color vision is governed by higher order mechanisms.

Methods

We used a noise-masking paradigm to measure chromatic discrimination thresholds in the $\Delta L/\Delta M$ plane of CC space. Here and in the following we use the more concise notation $\Delta L/\Delta M$ to denote the ($\Delta L/L$, $\Delta M/M$) plane of CC space. We investigated two conditions of "high noise contrast" and "low noise contrast" with maximum contrast values of 0.4 and 0.05, respectively, measured as the vector length in CC space.

Observers viewed a noise texture of 16 by 16 randomly flickering squares. A signal texture of 12 by 3 randomly flickering squares was added to the noise, and the observers had to indicate the orientation of the signal (horizontal or vertical) by pressing a corresponding button. The signal contrast was the dependent variable, i.e., the quantity to be measured.

The colors of the squares in the noise and signal texture were independently and randomly sampled from two lines in the $\Delta L/\Delta M$ plane of CC space, the "noise sampling line" and the "signal sampling line." It is known that such single-axis or "one-sided noise" (Hansen & Gegenfurtner, 2006) results in a narrowing of the tuning width of the noise-masking curves due to off-axis looking (D'Zmura & Knoblauch, 1998). Off-axis looking narrows the measured tuning width of the noise-masking curves but cannot introduce selective masking; i.e., it cannot introduce artificial peaks in the noise-masking curves. In the present study we used single-axis noise to keep the stimulus as simple as possible for the quest of the *number* of higher order mechanisms. To measure noise-masking curves for a particular noise direction, the direction of the noise sampling line was fixed and the direction of the signal sampling line was varied. A noise-masking curve thus corresponds to a fixed chromatic direction of the noise and shows how the threshold for detecting a signal varies depending on the direction of the signal relative to the noise. In other words, to measure a noise-masking curve, the noise was fixed and the signal varied. This is equivalent to the "vary signal" condition in Hansen and Gegenfurtner (2006). One could also employ a "vary noise" condition by fixing the signal direction and varying the noise direction. We have shown that both conditions result in the same thresholds contours for stimuli of equal noise amplitude in DKL space (Hansen & Gegenfurtner, 2006). We assumed that this property is independent of the

color space used to specify the stimuli and exclusively used the "vary signal" condition in the present study.

The sampling lines for signal and noise were centered at the origin of the $\Delta L/\Delta M$ plane such that their mean field was zero for all chromatic directions of the sampling line.

In Hansen and Gegenfurtner (2006) we specified the stimuli to have equal noise contrast in DKL space, while in the present study we specified the stimuli to have equal noise contrast in CC space. Because of these different definitions of the noise contrasts our previous results in DKL space could not simply be replotted in CC space.

The noise-masking paradigm

Masking noise leads to a linear increase in threshold contrast along the achromatic L/M/S direction (Pelli, 1981; Legge, Kersten, & Burgess, 1987) and along the isoluminant L/M direction (Gegenfurtner & Kiper, 1992). When signal and noise are modulated along different cardinal directions, the noise has no masking effect. This fact has been used to investigate chromatic mechanisms by systematically measuring noise-masking curves in different planes of DKL space (Gegenfurtner & Kiper, 1992; Li & Lennie, 1997; D'Zmura & Knoblauch, 1998; Stromeyer et al., 1999; Goda & Fujii, 2001; Lindsey & Brown, 2004; Hansen & Gegenfurtner, 2006; Cass et al., 2009) or CC space (Sankeralli & Mullen, 1997; Giulianini & Eskew, 1998; Stromeyer et al., 1999).

The noise-masking paradigm allows one to test the predictions of color models that differ in the number of mechanisms by measuring noise-masking curves for carefully chosen noise and signal directions.

If the signal and the noise are aligned, i.e., modulated along the same direction, both a model having only second-stage mechanisms and a model with higher order mechanisms predict maximum masking, i.e., maximum threshold elevation (Figure 3, rows 1 and 3). Both models also predict that the threshold gradually decreases as the signal directions deviates from the noise direction. The predictions however differ when the signal direction is chosen such that (a) it is modulated orthogonal to a putative mechanism that is aligned with the noise direction and (b) the projections of both the signal and the noise onto the cardinal axes are the same (Figure 3, rows 2 and 4). A model with second-stage mechanisms would predict the same response as if the signal were aligned with the noise, i.e., maximal masking (Figure 3, row 2). A model with multiple mechanisms would predict a reduced masking effect that could even drop to zero if a mechanism exists that is perfectly aligned with the signal and thus completely unaffected by the noise modulated along an orthogonal direction (Figure 3, row 4). In the

example given in Figure 3, the second-stage mechanisms are affected by the noise (gray bold lines) that masks the signal (orange bold lines), but a pair of higher order mechanisms along the main diagonal is completely unaffected by the noise. These higher order mechanisms can thus detect the signal as though no noise was present. Here we use the term "orthogonal" to refer to a relation between stimuli (or lights) and mechanisms. While angles between two chromatic directions or angles between two mechanisms vary depending on the color space, the relation between lights and mechanisms is independent of color space. A stimulus that is orthogonal to a mechanism is orthogonal to this mechanism in any color space. "Orthogonal" is thus a well-defined term. See also the section "Stimuli, mechanisms, orthogonality and the dual space" in the Discussion.

In the present study we used this paradigm to investigate the tuning of chromatic mechanisms in the $\Delta L/\Delta M$ plane of CC space.

Apparatus

Stimuli were displayed on a SONY GDM F520 color CRT monitor that was driven by a Bits++ digital-to-analog converter that provided an intensity resolution of 14 bits for each channel (Cambridge Research Systems, Cambridge, MA). The refresh rate of the monitor was 75 Hz non-interlaced. To linearize the relationship between output voltage and luminance, the lookup tables for each of the three monitor primaries were generated with a resolution of 14 bits using the OptiCal photometer and the provided calibration routines (Cambridge Research Systems, Cambridge, MA). All displays had a space-time averaged luminance of 51.2 cd/m^2.

A Photo Research PR-650 spectroradiometer (Photo Research, Chatsworth, CA) was used to measure the spectra of the red, green and blue phosphors at maximum intensity. The spectra were multiplied with the CIE 1931 color matching functions, as revised by Judd (1951) (see Wyszecki & Stiles [1982], table 1[5.5.2] or Stockman [2007]), to derive CIE x, y chromaticity coordinates and the luminance Y of the phosphors (Irtel, 1992). All further references to luminance and photometric luminance refer to the V(λ) curve as modified by Judd (1951).

The xyY coordinates of the monitor primaries measured at maximum intensity were 0.59549, 0.34584, and 27.421 (red); 0.28202, 0.59421, and 68.459 (green); and 0.16353, 0.09143, and 11.205 (blue).

Color spaces

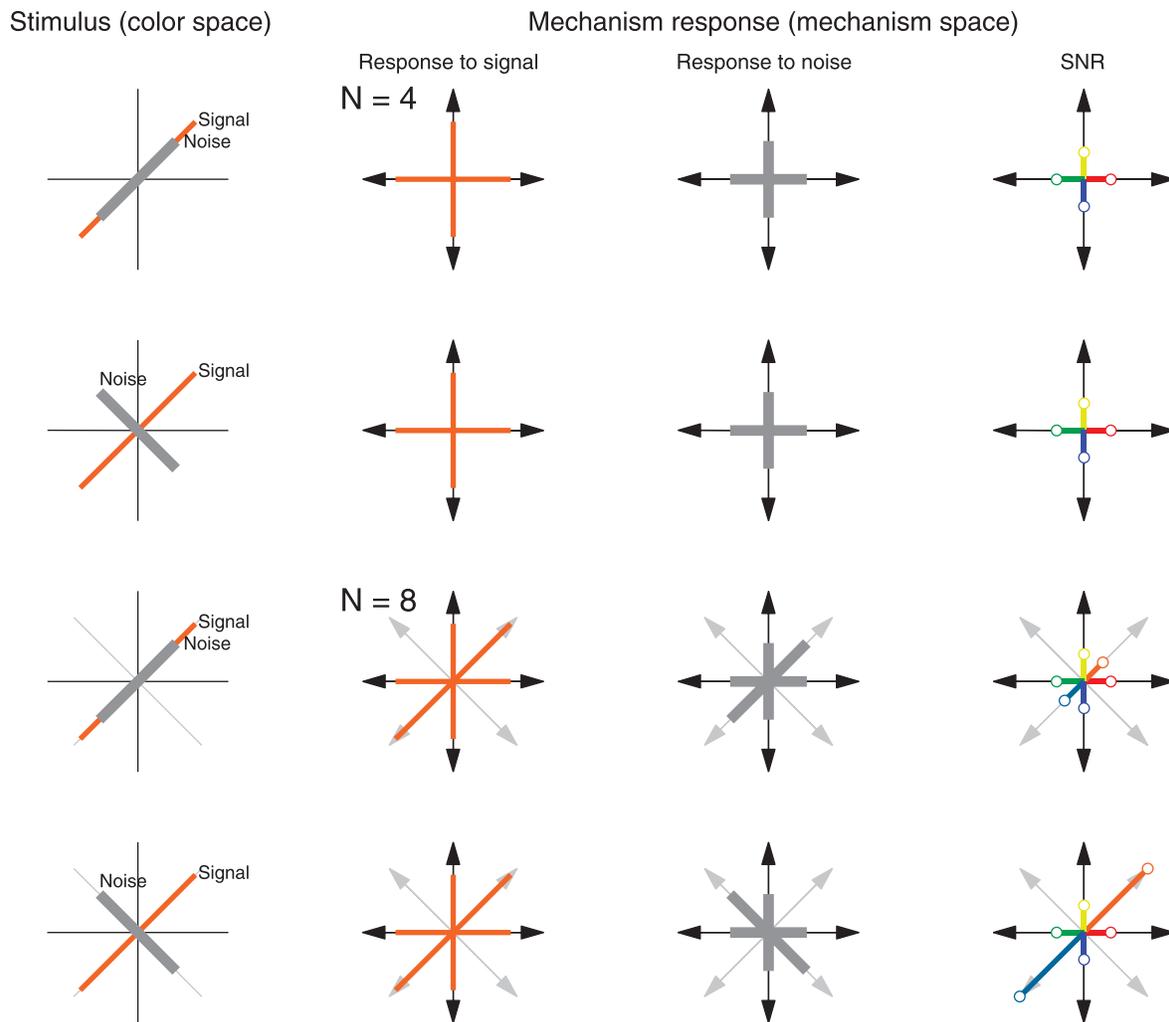We used two color spaces in this study, CC space and DKL space. We used DKL space to define the

Figure 3. Responses of a second-stage model ($N = 4$, rows 1 and 2) and a model with higher order mechanisms ($N = 8$, rows 3 and 4) to two different stimuli (aligned and orthogonal noise). The stimuli have a signal (orange) modulated along an intermediate direction and a noise (gray) modulated either along the same direction as the signal (aligned noise, first column, rows 1 and 3) or along an orthogonal direction (first column, rows 2 and 4). The second-stage model ($N = 4$) predicts the same response to the two different stimuli because in both cases the projections onto the second-stage mechanisms are the same (orange, signal, second column; gray, noise, third column) such that the signal-to-noise ratio is the same for all mechanisms (rows 1 and 2, fourth column). A model with higher order mechanisms ($N = 8$) can differentiate between the two different stimuli because the responses of the higher order mechanisms differ: the two unipolar mechanisms along the main diagonal are exclusively activated by the signal but unaffected by the orthogonal noise, resulting in a high signal-to-noise ratio for these mechanisms (fourth row, fourth column).

signal and noise directions that led to selective masking in previous work. We converted these directions to CC space and used CC space to specify the stimuli for our experiments such that they had equal CC. We show measured noise-masking curves both in CC and DKL space to compare the results with previous work.

CC space

Stimuli colors were chosen from the $\Delta L / \Delta M$ plane of CC space. The monitor spectra of the RGB primaries measured at full intensity were multiplied with the Smith and Pokorny (1975) cone fundamentals to calculate absorptions and contrasts in the L, M, and

S cones. Newer, more accurate cone fundamentals exist (Stockman & Sharpe, 2000), but under the conditions of our experiments the exact choice of cone fundamentals was not critical. Most importantly, we investigated CCs only, not absolute cone excitations. Converting our data based on the Stockman and Sharpe (2000) fundamentals led to negligible differences in CCs and no visible differences in the noise masking curves.

DKL space

The DKL color space (Krauskopf et al., 1982; Derrington et al., 1984) is based on the MacLeod and

Signal 15 deg$_{DKL}$ 45 deg$_{DKL}$ 75 deg$_{DKL}$
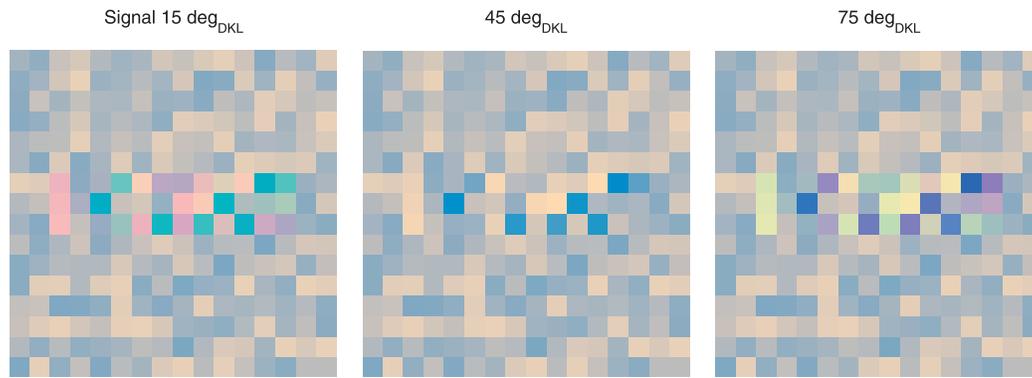

Figure 4. Sample stimuli for a fixed direction of the noise (45 deg$_{DKL}$) and varying directions of the signal (−30, 0, and +30 deg$_{DKL}$ with respect to the noise direction). In a given trial the signal was oriented either horizontally or vertically and the observer had to press a button to indicate the orientation.

Boynton (1979) chromaticity diagram and is derived from CC space. Both DKL and CC space are color spaces in which color values are defined relative to a reference color. This reference color represents the adapting field and defines the neutral gray point. Two chromatic axes intersect at this point and span an isoluminant plane. All lights in this plane have the same luminance as defined by the V(λ) photopic luminosity function modified by Judd (1951). Modulation along the L/M axis changes the excitations of the L and M cones such that their sum (luminance) is constant. Modulations along the L/M axis keep the excitation of the S cones constant and are thus invisible to the S cones. Lights along this axis vary between cherry and teal, a bluish-green. Modulations along the S axis change only the excitation of S cones and are invisible to L and M cones; modulations along this axis are thus confused by a tritanopic observer. Lights along this axis vary between lime and violet.

In the present study the axes of the DKL space were normalized in a device-dependent way such that 1 and −1 correspond to the maximum excursion along each axis within the gamut of the monitor. Consequently, the units on the axes and the chromatic angles are device dependent. The distance of a point in DKL space from its origin can be quantified independent of the device in terms of CCs (Smith & Pokorny, 1975). For the monitor used, modulating lights along the L/M axis resulted in an L-CC of 7.63% and an M-CC of 14.35%. Modulating lights along the S axis resulted in 80.61% S-CC. Along the L/M/S axis, all three types of cones were modulated up to values of 100% contrast. Further details are given in Appendix B: Definition of the DKL color space.

Stimuli and paradigm

Observers viewed a 16 by 16 pattern of dynamic random squares of 8 by 8 deg visual angle, such that each square subtended 0.5 deg visual angle. Each trial started with a blank gray screen shown for 500 ms, followed by the stimulus presentation of 10 frames of different noise patterns modulated at a frequency of 15 Hz, followed again by a blank screen for 500 ms. The noise squares were independently modulated along a particular direction in color space. Colors of the noise pattern were uniformly distributed along a single direction in color space. At each frame the noise value of a given square was drawn at random from the noise vector, independently across squares. Sample stimuli generated for a fixed direction of the noise and three signal directions are shown in Figure 4.

Signals were modulated along three noise directions at 39, 45, or 51 deg$_{CC}$ with a maximum chromatic contrast of 0.4. Contrast was defined as the vector length in CC space. These noise directions have been chosen because they map to equally spaced elevations of 45, 90, and 135 deg$_{DKL}$ in the plane spanned by the cardinal directions L/M and L/M/S. The idea that guided our choice of stimuli was to choose chromatic directions in CC space in such a way that these directions are well separated when transformed to DKL space (Figure 5).

In this way, different chromatic mechanisms can be stimulated. The experiment is identical to the experiment "Tuning in the L − M luminance plane, one-sided noise" reported in Hansen and Gegenfurtner (2006, p. 245–246), except that in the present work the contrast of the noise was set to 0.4 in the ∆L/∆M plane of CC space while in the 2006 article it was set to 0.4 in the "L − M/Lum plane," i.e., the plane spanned by the cardinal directions L/M and L/M/S.

The signal consisted of a rectangle of 12 by 3 squares that was added to the noise. The signal was oriented either horizontally or vertically and consisted of flickering squares modulated along one direction of color space. The signal squares were spatially and temporally aligned to the noise squares, excluding the
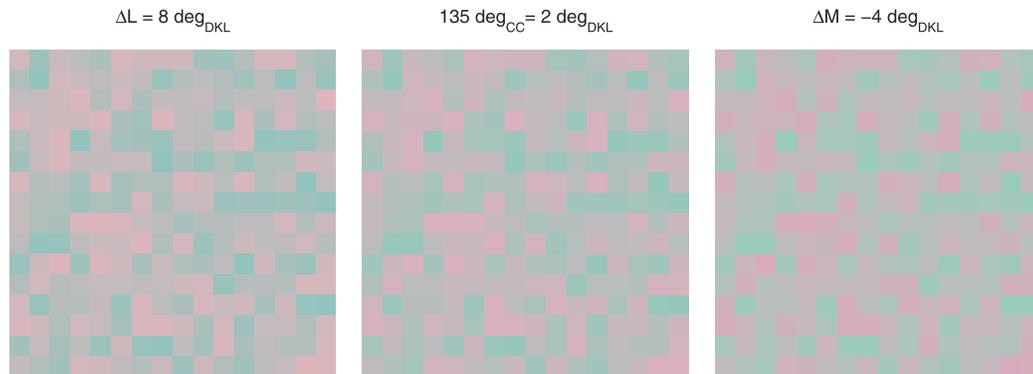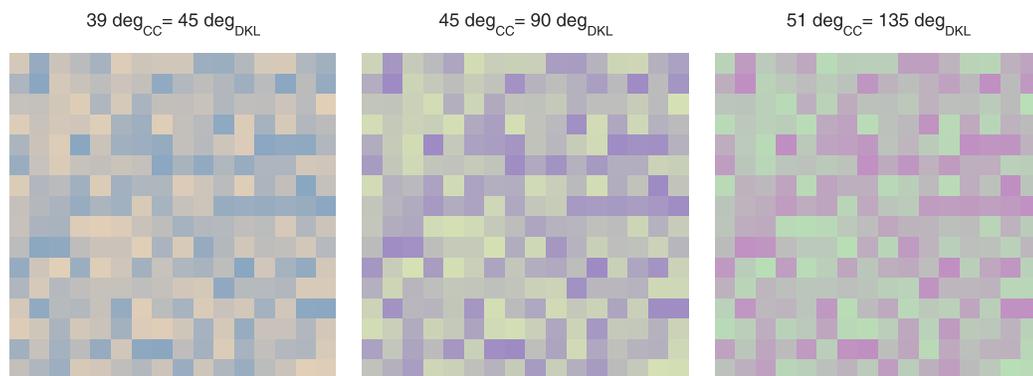
Figure 5. Rendering of noises patterns for different chromatic directions. Top row: The three noise directions ΔL (0 deg$_{CC}$), ΔM (90 deg$_{CC}$), and 135 deg$_{CC}$ used by Giulianini and Eskew (1998) are perceptually almost identical and fall close to the cardinal L − M direction. Bottom row: noise directions used in the present experiment are specified at equidistant directions in DKL space (45, 90, and 135 deg$_{DKL}$) and are perceptually clearly different. Note that the noise patterns are rendered with the spatial layout of the stimuli of the present study; Giulianini and Eskew (1998) used stimuli with a different spatial layout (concentric rings) and a different type of noise type (binary noise).

possibility of phase offsets that may mediate segmentation performance (Stromeyer et al., 1999). Noise and signal color directions were independently varied, as was the contrast of the noise. For each signal and noise combination, the signal contrast was measured at which the observer could reliably indicate the orientation of the signal rectangle.

Both the signal and the noise were symmetric modulations around the neutral gray point. Therefore, stimuli specified for directions α and α ± 180 deg are identical. In the polar plots in the Results section we follow common standards and duplicate each measured point by mirroring at the origin. To measure noise-masking curves for a particular chromatic direction, we kept the direction of the noise fixed and varied the direction of the signal relative to the noise. In a single run of the experiment we measured the noise-masking curve for a fixed noise direction with different signal directions randomly interleaved. We measured noise-masking curves for three noise directions (39, 45, and 51 deg$_{CC}$, corresponding to 45, 90, and 135 deg$_{DKL}$) by

determining discrimination thresholds for eight different signal directions with offsets −60, −30, −15, 0, 15, 30, 60, and 90 deg$_{DKL}$ relative to the noise direction. A standard up-down staircase method (Levitt, 1971) was used in a two-alternative forced-choice paradigm to measure the discrimination thresholds by adjusting the signal contrast. Each staircase terminated after six reversals.

Prior to the staircase procedure, preliminary thresholds were determined by decreasing the amplitude of the signal in geometrically smaller steps until the observer could no longer indicate the correct orientation of the signal. During the preliminary threshold procedure, observers could press a third button indicating "don't know," which triggered a half-way increase of the signal amplitude. Thresholds were determined as the mean of the six reversal points. Because we determined preliminary thresholds, the staircase already started close to the threshold. We thus assumed that even the initial reversals were close to the threshold to be estimated and need not to be discarded,
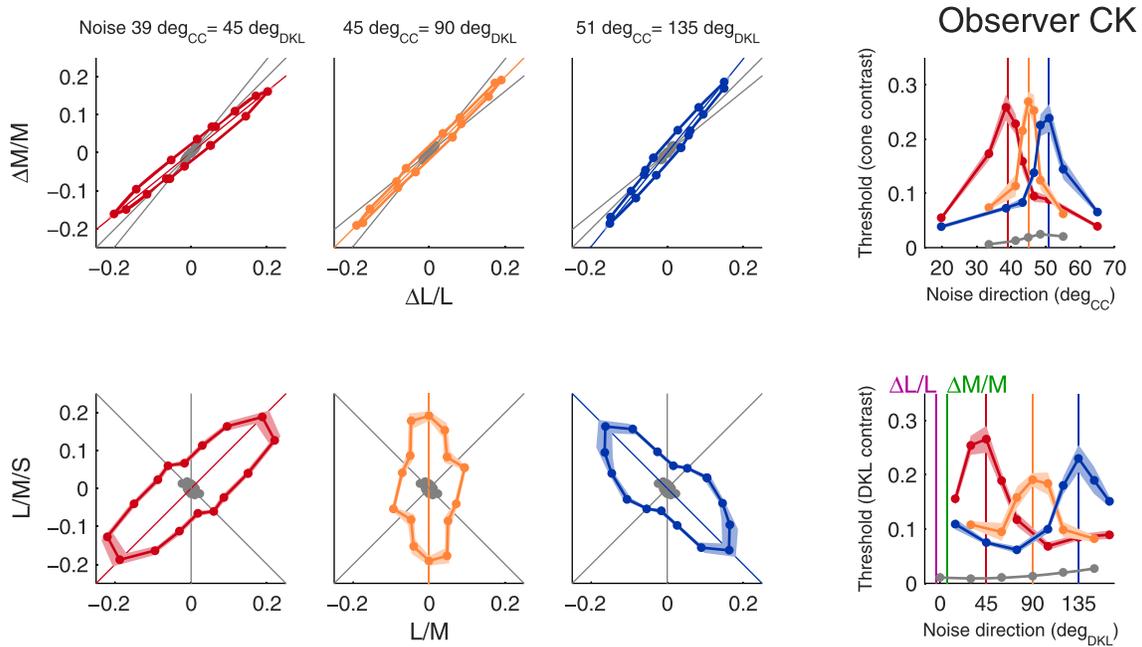
Figure 6. Noise-masking curves for observer CK in the ΔL/ΔM plane of CC space show selective masking. The curves show the threshold elevation for three different noise directions (39, 45, and 51 deg$_{CC}$ corresponding to 45, 90, and 135 deg$_{DKL}$ indicated by red, yellow, and blue lines, respectively; the colors were chosen for visualization only and do not necessarily resemble any of the colors along the chromatic direction of the noise). Gray curves denote the detection threshold in the absence of noise. Light shaded areas around each curve denote ±1 SEM. The same data is plotted in four different ways: in CC space (top row) and DKL space (bottom row), either in polar (columns 1–3) or cardinal format (column 4). In the polar plots half of the data points are duplicated by point reflection at the origin to generate a closed threshold contour. The purple and green vertical lines in the lower right panel indicate the position of the ΔL/L and ΔM/M axes of CC space in DKL color space. The data show some variations but follow a common pattern: masking is strongest at or near the noise direction and declines with increasing distance between the signal and the noise directions.

as commonly suggested (Falmagne, 1986; Stevens, Yantis, & Pashler, 2004).

Observers

One author (TH) and nine naïve observers (AM, CK, DW, JB, KD, KS, LV, MT, SW) with normal color vision and normal or corrected-to-normal visual acuity participated in this study. A subset of these observers participated in the low-contrast experiment (TH, CK, DW, JB). There were no systematic differences in results between the different observers.

Results

We measured noise-masking curves in the ΔL/ΔM plane of CC space. In the first series of experiments we used high-contrast noise, and in the second series of experiments we used low-contrast noise.

Evidence for multiple mechanisms with high-contrast noise

We have measured noise masking curves in the ΔL/ΔM plane of CC space for noise that was modulated along three directions (39, 45, and 51 deg$_{CC}$). The directions have been chosen because they map to equally spaced direction of 45, 90 and 135 deg$_{DKL}$ in DKL space. Polar and Cartesian plots of the noise masking curves of a single observer, plotted both in CC and DKL space are shown in Figure 6. Cartesian plots of the noise masking curves for all observers are shown in Figure 7. Each curve shows for a fixed noise direction how the threshold changes depending on the direction of the signal. The general pattern is a unimodal curve that peaks when signal and noise are modulated along the same direction, and sharply drops off as the signal deviates from the noise direction. Some curves do not follow this general pattern, having a broader, more plateau-like peak (e.g., noise direction 45 deg$_{DKL}$ for AM and DW), or having a bimodal distribution with a smaller, less pronounced maximum (e.g., noise direction 135 deg$_{DKL}$). The reason for these individual variations is unclear. We think that these
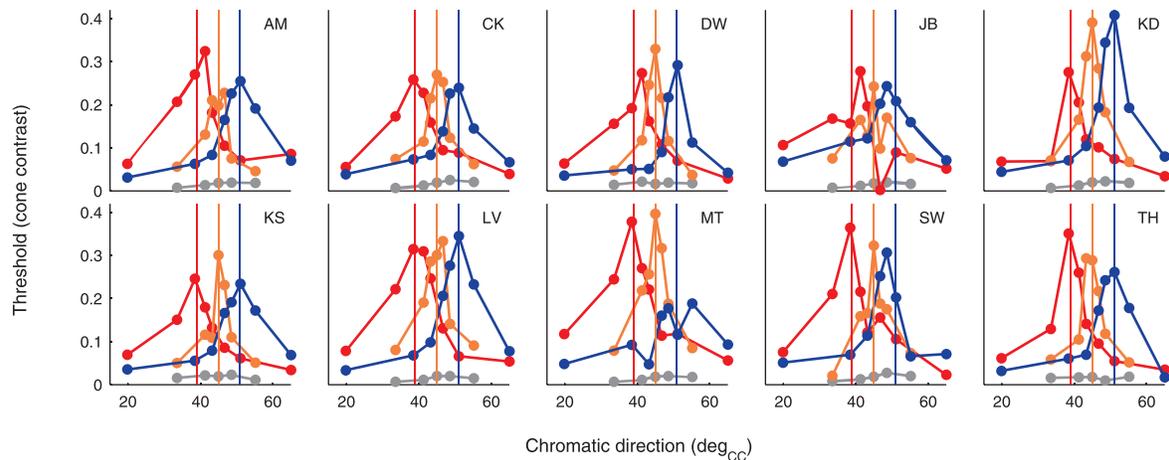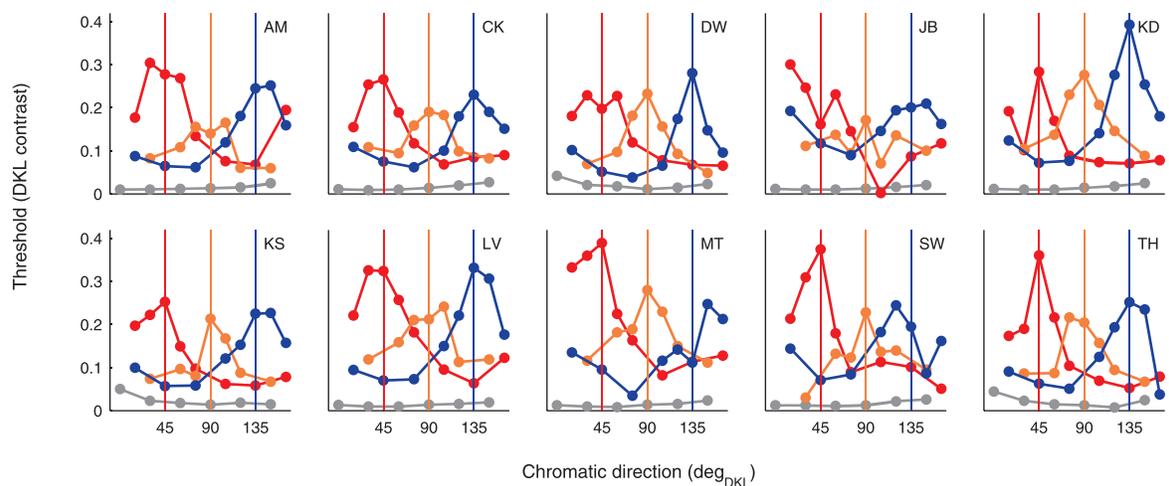
Figure 7. Cartesian plots of the noise-masking curves for all observers. The noise-masking curves follow a general pattern: Threshold elevation is highest when the noise is modulated along the same direction as the signal.

variations are unsystematic and irrelevant for the question studied here.

Overall, the noise-masking curves for each of the three different noise directions were remarkably consistent. We found no difference between signals modulated at cardinal versus noncardinal directions. In almost all cases, thresholds were highest when signal and noise were modulated along the same direction and rapidly declined with increasing separation in color direction between signal and noise.

As discussed above in the section "The noise-masking paradigm," a critical condition is the effect of an intermediate signal direction that (a) has the same projection on the second-stage mechanisms as a signal aligned with the noise and (b) is orthogonal to a putative higher order mechanisms along the noise direction. We refer to such a signal as "orthogonal" in contrast to an "aligned" signal that is modulated along the direction as the noise. A model with second-stage mechanisms only would predict the same discrimination thresholds for aligned and orthogonal signals, because the projections of both signals on the second-stage mechanisms are the same. A model with multiple mechanisms would predict a reduced effect of the noise and a decrease of the discrimination threshold for orthogonal signals. The threshold could even drop to zero if there is a higher order mechanism that is precisely aligned with the signal and thus unaffected by the noise that is modulated along a direction orthogonal to this mechanism.

We found that the thresholds for orthogonal signals were lower than the thresholds for aligned signals, falsifying the model with second-stage mechanisms only and indicating multiple higher order mechanisms. The individual thresholds of each observer for aligned and orthogonal signals for two intermediate noise directions (45 deg$_{DKL}$ and 135 deg$_{DKL}$) are depicted in Figure 8. Except for a single case (observer MT, 135 deg$_{DKL}$), both thresholds were different.
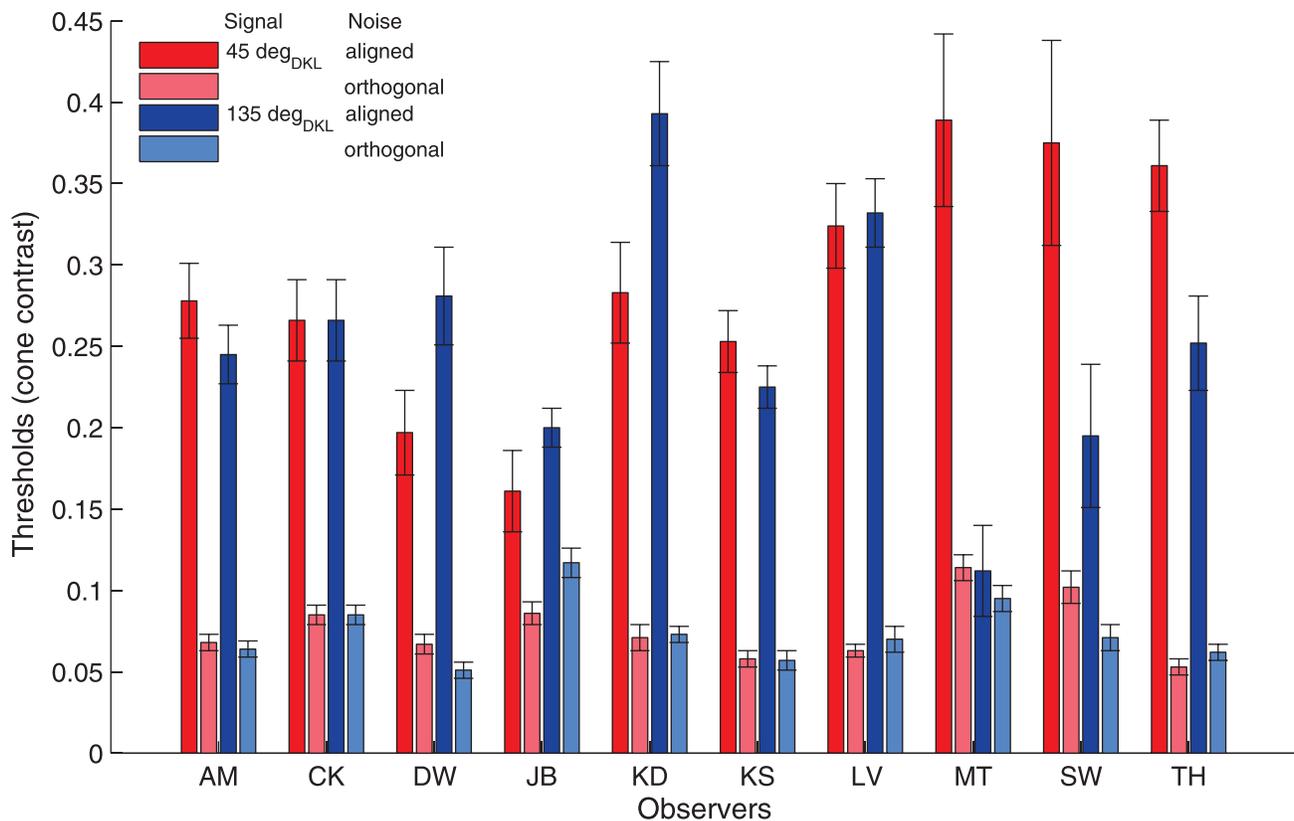
Figure 8. When the noise was modulated at intermediate directions (45 deg$_{DKL}$, red and 135 deg$_{DKL}$, blue), thresholds for aligned and orthogonal signals are different, indicating higher order mechanisms. All data share this pattern except for a single case (observer MT, noise direction 135 deg$_{DKL}$).

We also determined noise-masking curves in the $\Delta L/\Delta M$ plane averaged across 10 observers (Figure 9). Averaged data showed no systematic differences to the data obtained for a single observer. Noise-masking curves were narrow, and thresholds for orthogonal signals were lower than those for aligned signals. For noise modulated along intermediate directions in DKL color space this pattern is a clear indicator of multiple mechanisms.

The average detection thresholds in the presence of noise were elevated for all directions of the signal compared to the no-noise condition. This is different from previous findings in which detection thresholds in the presence of noise dropped to the no-noise condition when the signal was modulated orthogonal to the noise (Hansen & Gegenfurtner, 2006). The reason for this discrepancy is unclear.

Overall we found narrow noise-masking curves with highest thresholds for aligned and lowest thresholds for orthogonal signal directions, indicating higher order mechanisms. Noise-masking curves were significantly different for each chromatic direction of the noise. In previous work we obtained similar curves as part of a more complete data set, and we have shown with a quantitative model that such different noise-masking curves are inconsistent with a model that only has

second-stage mechanisms but consistent with a model that has multiple broadly tuned higher order mechanisms (Hansen & Gegenfurtner, 2006).

No evidence for multiple mechanisms with low-contrast noise

We also ran the experiment with a lower contrast of the noise (0.05 instead of 0.4). In this case, we failed to find evidence for selective masking (Figure 10). This is an important point that shows that signals must be sufficiently large to activate higher order mechanisms. Cone contrasts of the noise below 0.05 have also been used by Giulianini and Eskew (1998), who failed to find evidence for multiple higher order mechanisms. Medium CC values of 0.1888 and 0.222 have been used by Stromeyer et al. (1999), who found no clear evidence for selective masking when spatial phase shifts are eliminated.

One feature of the results is that when thresholds are plotted in DKL space, they are elevated relative to no-noise in some noncardinal directions, e.g., 45 and 90 deg$_{DKL}$, for all noise angles. The reason for this is unclear.

Here we found no differences in thresholds between aligned and 90 deg$_{DKL}$ away signals when the contrast
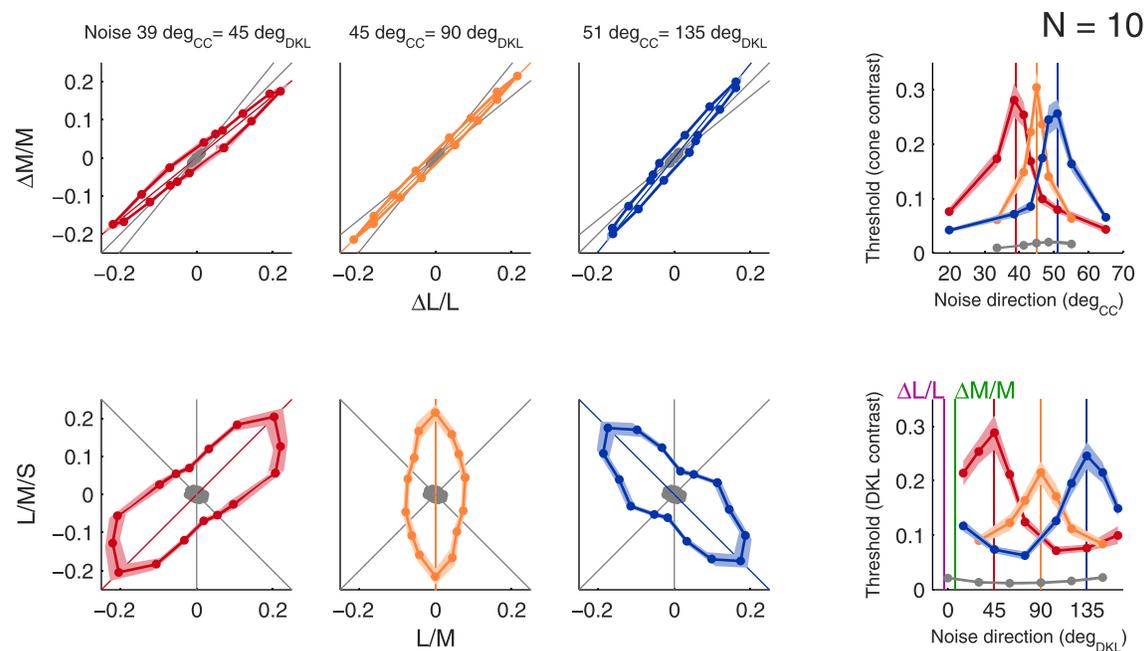
Figure 9. Mean of noise-masking curves for $N = 10$ observers show selective masking, consistent with multiple higher order mechanisms. Format is the same as in Figure 6.

was low. For a noise modulated along a direction of 45 deg_{DKL}, the average thresholds were 0.034 ± 0.004 for aligned and 0.034 ± 0.003 for orthogonal signals; for noise modulated along a direction of 135 deg_{DKL}, the average thresholds were 0.035 ± 0.004 for aligned signals and 0.030 ± 0.002 for orthogonal signals.

Discussion

We measured noise-masking curves for noise modulated along three different directions in CC space and found selective masking. We interpret this as evidence for higher order color mechanisms. When the noise amplitude was low—just above threshold—we found no evidence for selective masking.

By now, the work on higher order mechanisms has a long history. Eskew (2009) reviewed 25 years of research on higher order color mechanisms and made a tremendous effort to discuss dozens of studies. Although Eskew (2009, p. 2686) admitted that "the bulk of evidence has been taken to support the existence of multiple, linear color mechanisms," he concluded that "no consensus on higher order mechanisms has been reached." What is the reason for this discrepancy? All studies that specified their stimuli in CC space interpreted their findings as being inconsistent with multiple higher order mechanisms. CC space is the color space exclusively used in studies from the lab of Eskew, and in his review Eskew (2009) focused

on studies that specified their stimuli to have equal noise power when represented in CC space.

We will try to explain in detail the reason why previous studies in CC space failed to find evidence for multiple mechanisms. In brief, studies in CC space used noise directions that stimulated only a single higher order mechanism. The reason why this major limitation was not immediately obvious is because of the highly nonlinear mapping of angles from CC to DKL space. The stimuli chosen in previous studies in CC space were well separated in CC space, but mapped to virtually the same angle in DKL space. Previous results indicate that higher order chromatic mechanisms are approximately evenly spaced in DKL space. Studies in CC space thus used stimuli that tapped into only a single second-stage mechanism, and they consequently failed to find evidence for higher order mechanisms.

The choice of color space for studying higher order mechanisms

Many studies have used CC space to specify their stimuli when investigating higher order mechanisms. The rationale for this choice is not immediately clear, since the neural correlate of higher order mechanisms is in the cortex, and the input to the cortex is organized not along the $\Delta L/L$, $\Delta M/M$, and $\Delta S/S$ axes of CC space, but rather the cardinal axes of DKL space. DKL space thus seems to be the natural choice for the investigation of higher order mechanisms, just as CC
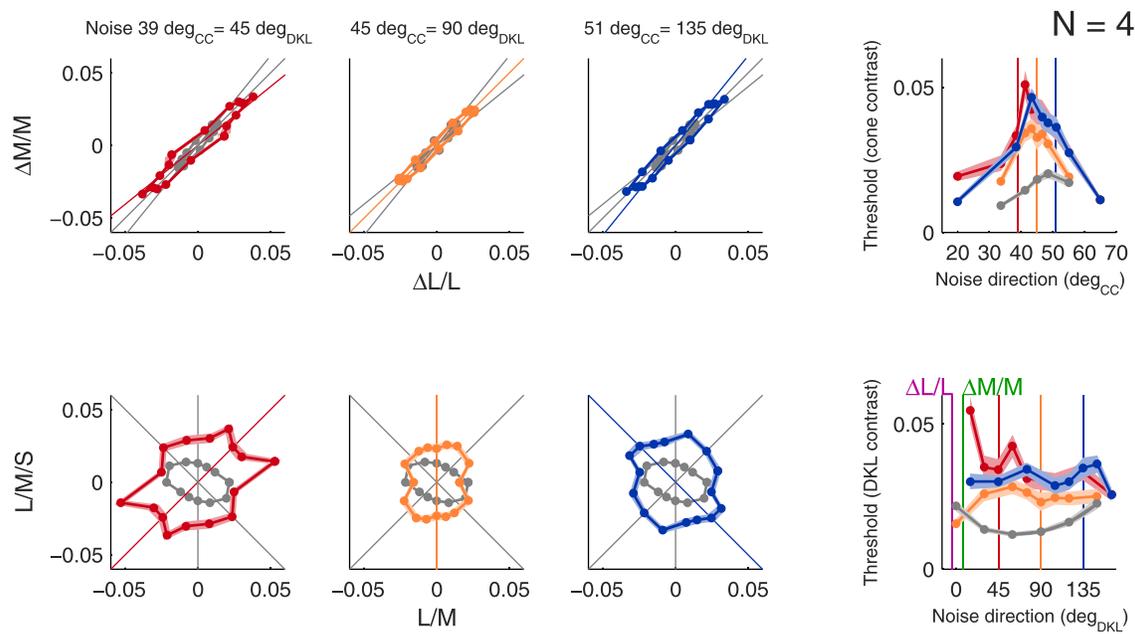
Figure 10. Mean of noise-masking curves for $N = 4$ observers show no selective masking, when the contrast of the noise was low. Format of the figure is the same as Figure 6, but the scale is about three times smaller.

space seems to be the proper choice for studying the cone inputs to the second order mechanisms.

So why may CC space have been chosen to study higher order mechanisms? First, CC space is a contrast space that incorporates a simple mechanism for first-site adaptation. However, this is irrelevant in the present context because the adapting chromaticity is typically held constant in studies of higher order mechanisms, including the present. Further, having a simple adaptation mechanism is not an advantage of CC over DKL space because a similar mechanism can be incorporated in DKL space too (Brainard, 1996).

Second, CC space is well-defined, and thus the units along the axes of CC space are well-defined. In contrast, there is no standardization of DKL space: Only the axes of DKL space, i.e., the cardinal directions, are defined, but the relative scaling of the axes is not. The axes of DKL space are scaled either in multiples of detection threshold (which depends on observers, stimuli, and methods) or by setting the maximum values along each axis to unity (which depends on the display). Both methods result in similar scaling of the axes across studies (because monitors are similar and observers' chromatic detection performances are similar). More importantly, DKL space is perceptually more uniform than CC space because detection and discrimination contours are more circular in DKL space (Krauskopf & Gegenfurtner, 1992; Hansen, Giesel, & Gegenfurtner, 2008, their Figure 1). Indeed, if DKL axes are scaled in multiples of detection threshold, detection contours at the origin are circular by definition. In CC space, in contrast, detection contours at the origin are extremely elongated by a factor

of about 10 (Gegenfurtner & Hawken, 1996, their Figure 2; Stromeyer et al., 1999). Furthermore, DKL spaces closely resemble color spaces that were designed to be perceptually uniform such as Lab or Luv.

Let us hypothesize that higher order mechanisms are equally distributed in some higher order, i.e., perceptually roughly uniform color space. One study has provided some evidence that higher order color mechanisms are equally spaced in DKL color space: Hansen and Gegenfurtner (2006) tested a model with roughly equally spaced mechanisms that could account for their data. Mechanisms that are equally spaced in a perceptually highly uniform color space cluster in the perceptually highly nonuniform CC space. This nonlinear mapping of angles from a perceptually more uniform color space to CC space obscures the choice of suitable intermediate directions in CC space. For example, all angles in the second quadrant of the $\Delta L/\Delta M$ plane of CC space (between 90 and 180 $\deg_{CC}$) map to virtually the same angle in DKL space close to the $L - M$ axis. In some studies (Sankeralli & Mullen, 1997; Giulianini & Eskew, 1998) stimuli were defined at noise directions in CC space that were perceptually almost identical. All stimuli that were modulated along these perceptually almost identical noise directions stimulated almost exclusively the same pair of mechanisms. Consequently, these studies found *no evidence in favor of* higher order mechanisms and may have sometimes been viewed as providing *evidence against* such mechanisms.

To sum up, any perceptually highly uniform color space would be more suitable to study higher order mechanisms than the perceptually highly nonuniform

Hansen & Gegenfurtner

CC space. DKL space has the particular advantage of being the only color space whose axes are linked by definition to the second-stage mechanisms. We conclude that in DKL space stimuli are easier to define and results are easier to interpret when studying higher order color mechanisms.

Orthogonality between stimuli and mechanisms is preserved under linear transformations between color spaces: Stimuli, mechanisms, orthogonality, and the dual space

The fact that angles change dramatically when transformed from CC to DKL space has been noted previously. Sankeralli and Mullen (2001, p. 53) pointed out "that the angle between the colour direction of two stimuli depends on the space in which the stimuli are presented." However, they combined this simple fact with the wrong idea that the "orthogonality property is valid only for this space [i.e., CC space] or any orthonormal transformation of this space" (Sankeralli & Mullen, 2001, p. 55) to incorrectly criticize the use of sectored noise in DKL space by D'Zmura and Knoblauch (1998). From the incorrect proposition that the orthogonality principle is valid only in CC space, they argued that DKL space is not an orthonormal transformation of CC space (which is correct) and that the orthogonality principle cannot be applied in DKL space and consequently the data of their sectored noise experiments are misinterpreted by D'Zmura and Knoblauch (1998). Because the proposition is wrong (see following text), the whole argument is not valid.

Knoblauch and D'Zmura (2001) replied to Sankeralli and Mullen (2001) and pointed out that the relation between lights and neural mechanisms is independent of the choice of color space. Orthogonality is not a relation between lights or stimuli, but between stimuli and mechanisms. A light that is orthogonal to a mechanism remains orthogonal to that mechanisms in any color space used to represent the light. Consequently, the orthogonality principle is not limited to CC space. Instead, any color space can be used to investigate chromatic mechanisms. Most important, the results of the experiments by D'Zmura and Knoblauch (1998) remain valid, namely that detection is mediated by multiple broadly tuned chromatic mechanisms.

There is some confusion about if or how orthogonality is preserved under transformation of a color space. Because this is one of the issues that has repeatedly confused experts and novices alike, we will detail it in the following. Intuitively, the relation between stimuli (or lights) and mechanisms should be independent of the choice of the color space, and this is the case (Knoblauch & D'Zmura, 2001; Sankeralli &

Mullen, 2001). Orthogonality is not a relation between stimuli, but between stimuli and mechanisms. A stimulus (or light) that is orthogonal to a mechanism remains orthogonal to that mechanism in any color space that is used to represent the stimulus (or light). Because "we are defining a relation between lights and mechanisms" (Knoblauch & D'Zmura, 2001, p. 1683), and because mechanisms do not exist in the same space as stimuli (or lights), but in its *dual space*, mechanisms are transformed differently than stimuli (Krantz, 1975; Knoblauch, 1995, p. 1683): "A linear transformation of the color space in which lights are described induces a related but different transformation of the dual space of chromatic detection mechanisms." More precisely, if the stimuli are transformed by a matrix $\mathbf{A}$, then the mechanisms are transformed in the dual space by the transposed inverse of this matrix, i.e., by $(\mathbf{A}^{-1})^{\mathrm{T}}$.

If this is taken into account, Knoblauch and D'Zmura (2001) showed with basic linear algebra that orthogonality between a stimulus $\mathbf{s}$ and a mechanism $\mathbf{m}$ is preserved under a linear transformation by an invertible matrix $\mathbf{A}$. Formally, a stimulus and a mechanism are orthogonal to each other if their scalar product is zero:

$$\mathbf{s}^{\mathrm{T}}\mathbf{m} = 0.$$

Transforming a stimulus by left-multiplying it with matrix $\mathbf{A}$ requires a related transformation of the mechanism in the dual space by $(\mathbf{A}^{-1})^{\mathrm{T}}$. The scalar product of the transformed stimulus and the transformed mechanism is zero, so both remain orthogonal to each other after the transformation:

$$(\mathbf{As})^{\mathrm{T}}(\mathbf{A}^{-1})^{\mathrm{T}}\mathbf{m} = \mathbf{s}^{\mathrm{T}}\mathbf{A}^{\mathrm{T}}(\mathbf{A}^{-1})^{\mathrm{T}}\mathbf{m} = \mathbf{s}^{\mathrm{T}}\mathbf{m} = 0.$$

To sum up, orthogonality between stimuli and mechanisms is preserved under linear invertible transformations of color spaces. Consequently, the orthogonality principle is valid in any color space that is a linear transformation of CC space, and any such color space can be used to study chromatic mechanisms.

Selective masking as evidence for higher order mechanisms

Higher order mechanisms cannot be measured directly in psychophysical experiments. Selective masking along intermediate directions is regarded as a fingerprint of higher order mechanisms. However, alternative interpretations have been suggested.

Zaidi and Shapiro (1993, p. 416) defined two "third stage" mechanisms as a nonlinear combination of the second-stage mechanisms and showed that an adaptable linear interaction between these mechanisms can result in a pattern that resembles the adaptation data measured by Webster and Mollon (1991). However,

Zaidi and Shapiro ([1993](), p. 422) admitted that "In the response equalization process proposed here the shape of each response function is set by matching differential sensitivity to the relative frequency of the input levels. This process is optimal, but unrealistic in that it requires the visual system to extract the complete frequency distribution of input levels."

Another model has been proposed by Eskew ([2009]()) based on two linear and two nonlinear mechanisms that could account for the broad noise-masking curves observed by Hansen and Gegenfurtner ([2006]()) for two-sided noise. "However, this is not a complete model of the Hansen and Gegenfurtner results; this four-mechanism model does not a good job accounting for the results with single-sided noise" and if fact "in general this model does not a good job with any of the studies that have used 'single-sided' noises, whether the tuning is narrow or broad" (Eskew, [2009](), p. 2702).

In contrast, the model proposed by Hansen and Gegenfurtner ([2006]()) based on multiple linear mechanisms could account for their complete data set. Of course this is only one out of potentially numerous models that could fit the data, and of course a model fit cannot prove the existence of multiple higher order mechanisms. However, as long as no other model can account for the full data set, the model by Hansen and Gegenfurtner ([2006]()) based on multiple linear mechanisms is the most parsimonious and best explanation for the interactions at the third stage of color processing.

A critical review of psychophysical evidence against higher order mechanisms

We shall also review psychophysical studies the of higher order mechanisms that found no evidence for higher order mechanisms. All these studies defined their stimuli in CC space.

Stimuli specified in DKL space

All studies in which stimuli were specified in DKL color space found selective masking, providing evidence for higher order color mechanisms. Even in the classical study by Krauskopf et al. ([1982]()) on "Cardinal directions of color space" some evidence for higher order mechanism was reported, which was confirmed and underscored by a re-analysis and further experiments in a follow-up study (Krauskopf et al., [1986]()). Thus, all studies in DKL space are consistent with higher order mechanisms.

Stimuli specified in CC space

All studies that defined their stimuli in CC space tend to interpret their results as providing no evidence in favor of higher order mechanisms. All these studies were conducted by Mullen, Stromeyer, or Eskew.

Sankeralli and Mullen ([1997]()) used a noise-masking paradigm similar to the one pioneered by Gegenfurtner and Kiper ([1992]()) to investigate whether detection thresholds in the presence of noise could be accounted for solely by cardinal mechanisms. Sankeralli and Mullen ([1997]()) used stimuli in which the signal and the noise were confined to the $\Delta L/\Delta M$ plane of CC space. Four directions of the signal were used: 45 deg$_{CC}$ (L/M/S, achromatic), -45 deg$_{CC}$ (L/M, $\approx$ teal/cherry isoluminance), 0 deg$_{CC}$ (L cone direction, light red/dark green), and 90 deg$_{CC}$ (M cone direction, dark red/light green). Before investigating the noise-masking, Sankeralli and Mullen ([1997]()) tested the independence of the signal and noise directions, i.e., whether the detection of a signal modulated along one direction was independent of the amount of noise along another direction. They found independence between an iso-luminant signal and luminance noise (and vice versa), but not between $\Delta L/L$ and $\Delta M/M$ cone directions. When transformed to DKL it becomes evident that $\Delta L/L$ and $\Delta M/M$ are not independent, because they both map to directions close to L/M and thus stimulate the same mechanisms (L − M and M − L) (cf. [Figure 1]() and [Figure 2]()).

The stimuli used by Sankeralli and Mullen ([1997]()) were identical to the ones used by Gegenfurtner and Kiper ([1992]()), with the exception that static noise was used instead of dynamic noise. Sankeralli and Mullen ([1997]()) found a wider bandwidth of chromatic tuning. They interpreted their data as being consistent with three second-stage mechanisms. When using signals in intermediate directions of color space, they observed no masking for noise along orthogonal directions, which provides evidence for higher order mechanisms tuned to these intermediate directions (their Figure 9). In fact, Sankeralli and Mullen ([1997](), p. 2642) report that "The cosine model is a poorer fit to the data than in previous conditions; specifically, there is maximum masking for all three subjects when the noise is closest to the signal direction. This may suggest the presence of a weaker intermediate mechanism tuned to the signal direction, as proposed by Gegenfurtner and Kiper." However, they preferred an alternative interpretation based on "differential phase shifts as proposed by Chaparro et al.," (Sankeralli & Mullen, [1997](), p. 2642) although phase shifts occurred neither in their own stimuli nor in all stimuli used by Gegenfurtner and Kiper ([1992]()), except in a single control experiment. Later experiments confirmed that selective masking occurs in the absence of phase differences between signal and noise (Hansen & Gegenfurtner, [2006]()).

Giulianini and Eskew ([1998]()) used a noise-masking paradigm to characterize the postreceptoral mechanisms that mediate detection of stimuli in the $\Delta L/\Delta M$

plane of CC space. Chromatic masking noises of different chromaticities and spatial configurations were used, and threshold contours for the detection of Gaussian and Gabor tests were measured. The results did not show masking that was narrowly selective for the chromaticity of the noise. On the contrary, they found that detection of their tests was mediated only by two mechanisms, namely, the chromatically opponent L − M mechanism and a nonopponent luminance mechanism. Note that the stimulus size in the current study differs from the stimulus size in the study of Giulianini and Eskew (1998): The stimuli in the current study were 8 by 8 deg squares made up from 16 by 16 smaller homogeneously colored squares of 0.5 deg visual angle that were clearly visible, while the stimuli used by Giulianini and Eskew (1998) were concentric rings or lines of 2.64 min of visual angle, of alternating test and noise color. The rings or lines were not visible for the chromatically detected tests and only occasionally seen for the achromatically detected tests. Giulianini and Eskew (1998) interpreted these results as being inconsistent with the hypothesis of multiple chromatic mechanisms mediating detection in the $\Delta L/\Delta M$ plane of CC space. As detailed in the Introduction, the problem of this study was the choice of "different" noise directions in CC space that are no longer different at the postreceptoral level, but stimulated essentially only the L − M mechanism. The responses could thus be fitted by a model with only second-stage mechanisms, leading to the conclusion that only second-stage mechanisms exist.

Stromeyer et al. (1999) used sine waves for their signals and noise maskers. They found evidence for intermediate, higher level chromatic mechanisms whenever there were phase offsets between signals and noise and speculated that the selective masking observed by Gegenfurtner and Kiper (1992) might have been due to the spatial differences in signals and noise maskers. However, as noted above, this argument applies only to a single control experiment in the study of Gegenfurtner and Kiper (1992). In the main part of their paper, broadband spatio-temporal noise was used, which prevented the phase offsets hypothesized by Stromeyer et al. (1999). The finding of only moderate selective masking by Stromeyer et al. (1999) when no phase offset was present may be explained by the moderate contrast of the noise (0.222 for 55 deg$_{CC}$ or 0.188 for 34 deg$_{CC}$). Our results of a complete lack of selective masking for low-contrast noise suggests that the noise used by Stromeyer et al. (1999) was too low to result in clear selective masking.

Giulianini and Eskew (2007) used a method for testing the linearity of cone combination of chromatic detection mechanisms and applied it to S-cone detection. They found no evidence for multiple linear mechanisms. The stimuli were specified in the (L, M), (L, S), and (M, S) planes of CC space with maximal noise power at any given angle, i.e., the maximum contrast permitted by the monitor gamut. The reason for the failure to find multiple mechanisms is unclear but may be due to the large amount of noise energy at high spatial and temporal frequencies. The concentric noise rings in their experiments had a width of only 2.6 min and switched chromaticity with probability 0.5 at 16.8 Hz. The test was filled within the gaps of the noise rings. This stimulus is hardly visible, similar to the stimuli at threshold for the low-noise experiment in the present study, in which we also found no evidence for higher order mechanisms. Higher order mechanisms are probably only found when the stimuli are significantly above detection threshold.

Psychophysical evidence for higher order mechanisms

There are numerous studies using a variety of paradigms, from adaptation to noise masking and chromatic detection and discrimination, that all found evidence for higher order mechanisms.

Two classical studies used adaptation (or "habituation") and found evidence for higher order mechanisms (Krauskopf et al., 1982; Webster & Mollon, 1991). Note that Krauskopf et al. (1982) originally reported evidence only for two major second stage chromatic mechanisms along the cardinal axes. However, a reanalysis of their data revealed the existence of additional higher order mechanisms (Krauskopf et al., 1986).

Further evidence for multiple chromatic mechanisms was found by McKeefry, McGraw, Vakrou, and Whitaker (2004), using adaptation in a Vernier alignment task, and by McGraw, McKeefry, Whitaker, and Vakrou (2004), using positional adaptation.

Gegenfurtner and Kiper (1992) were the first to use a noise-masking paradigm. Using a Gabor pattern as signal embedded in spatio-temporal chromatic noise, they found evidence for multiple chromatic mechanisms. Numerous further studies that used variants of the noise-masking paradigm confirmed the finding of multiple chromatic mechanisms (Krauskopf & Gegenfurtner, 1992; Li & Lennie, 1997; D'Zmura & Knoblauch, 1998; Krauskopf, 1999; Goda & Fujii, 2001; Lindsey & Brown, 2004; Hansen & Gegenfurtner, 2006; Cass et al., 2009).

Giesel, Hansen, and Gegenfurtner (2009) measured discrimination thresholds for chromatically variegated stimuli and found that a model with eight mechanisms accounted for the effect of chromatic variation within the stimuli and provided a better fit to the discrimination thresholds than a four-mechanism model.

A complete recent list of studies providing evidence for multiple mechanisms can be found in the review by Eskew (2009).

Physiological findings

Psychophysical findings consistent with multiple higher order mechanisms agree well with results from cortical physiology. In cortical visual areas V1, V2, V3, and IT, neurons exhibit a large variety of different color preferences and are not limited to the cardinal directions (Lennie, Krauskopf, & Sclar, 1990; Komatsu, Ideura, Kaji, & Yamane, 1992; Gegenfurtner, Kiper, & Fenstemaker, 1996; Gegenfurtner, Kiper, & Levitt, 1997; Kiper, Fenstemaker, & Gegenfurtner, 1997; Komatsu, 1998; Wachtler, Sejnowski, & Albright, 2003; Conway et al., 2007; Conway & Tsao, 2009). The widths of the chromatic tuning curves of cortical neurons typically cover a range of values. In macaque V1, tuning widths vary between 10 and 90 deg (Wachtler et al., 2003). In V2, Kiper et al. (1997) found a bimodal distribution of tuning widths around 30 and 60 deg. In general, the proportion of narrowly tuned neurons increases along the hierarchy of processing stages (see Gegenfurtner, 2003, for a review). We suggest that a group of neurons of similar chromatic preference and tuning widths can be abstracted as a higher order mechanism.

Conclusions

We report selective chromatic masking at noncardinal directions for stimuli defined in CC space. Our results resolve the discrepancy between previous studies in CC space that found no evidence for higher order mechanisms and numerous studies in DKL space that did. Selective masking indicates higher order mechanisms, since so far no alternative model has been proposed; only one model based on multiple, broadly tuned higher order mechanisms accounts for the selective masking at cardinal and noncardinal directions and the variation of noise-masking curves based on the kind of noise (Hansen & Gegenfurtner, 2006). We conclude that cortical color vision is governed by higher order mechanisms.

Acknowledgments

Commercial relationships: none.
Corresponding author: Thorsten Hansen.
Email: Thorsten.Hansen@psychol.uni-giessen.de.
Address: Otto-Behaghel-Str. 10F1, 35396 Gießen, Germany.

References

Brainard, D. H. (1996). Cone contrast and opponent modulation color spaces. In P. K. Kayser & R. M. Boynton (Eds.), *Human color vision.* (appendix part IV, 2nd edition, pp. 563–579). Washington, DC: Optical Society of America.

Buchsbaum, G., & Gottschalk, A. (1983). Trichromacy, opponent colours coding and optimum colour information transmission in the retina. *Proceedings of the Royal Society of London (Series B, Biological Science)*, 220(1218), 89–113.

Cass, J., Clifford, C. W., Alais, D., & Spehar, B. (2009). Temporal structure of chromatic channels revealed through masking. *Journal of Vision, 9*(5):17, 1–15, http://www.journalofvision.org/content/9/5/17, doi:10.1167/9.5.17. [PubMed] [Article]

Conway, B. R., Moeller, S., & Tsao, D. Y. (2007). Specialized color modules in macaque extrastriate cortex. *Neuron, 56*(3), 560–573. [PubMed]

Conway, B. R., & Tsao, D. Y. (2009). Color-tuned neurons are spatially clustered according to color preference within alert macaque posterior inferior temporal cortex. *Proceedings of the National Academy of Sciences (USA), 106*(42), 18034–18039. [PubMed] [Article]

Dacey, D. M. (2000). Parallel pathways for spectral coding in primate retina. *Annual Reviews in Neuroscience, 23,* 743–775.

De Valois, R. L., De Valois, K. K., & Mahon, L. E. (2000). Contribution of S opponent cells to color appearance. *Proceedings of the National Academy of Sciences (USA)*, 97(1), 512–517. [PubMed] [Article]

Derrington, A. M., Krauskopf, J., & Lennie, P. (1984). Chromatic mechanisms in lateral geniculate nucleus of macaque. *Journal of Physiology, 357,* 241–265. [PubMed] [Article]

D'Zmura, M., & Knoblauch, K. (1998). Spectral bandwidths for the detection of color. *Vision Research*, *38*(20), 3117–3128.

Eskew, R. T., Jr. (2008). Chromatic detection and discrimination. In R. H. Masland & T. D. T. D. Albright (Eds.), *The senses: A comprehensive reference of vision.* (Vol. 2, pp. 101–117). New York: Academic.

Eskew, R. T., Jr. (2009). Higher order color mechanisms: A critical review. *Vision Research, 49*(22), 2686–2704.

Falmagne, J.-C. (1986). Psychophysical measurement and theory. In K. Boff, L. Kaufman, & J. Thomas (Eds.), *Handbook of perception and human performance*. New York: John Wiley.

Gegenfurtner, K. R. (2003). Cortical mechanisms of colour vision. *Nature Reviews Neuroscience*, *4*(7), 563–572.

Gegenfurtner, K. R., & Hawken, M. J. (1996). Interaction of motion and color in the visual pathway. *Trends in Neurosciences, 19,* 394–401. [PubMed]

Gegenfurtner, K. R., & Kiper, D. C. (1992). Contrast detection in luminance and chromatic noise. *Journal of the Optical Society of America (A)*, *9*(11), 1880–1888.

Gegenfurtner, K. R., Kiper, D. C., & Fenstemaker, S. B. (1996). Processing of color, form, and motion in macaque area V2. *Visual Neuroscience*, *13*(1), 161–172.

Gegenfurtner, K. R., Kiper, D. C., & Levitt, J. B. (1997). Functional properties of neurons in macaque area V3. *Journal of Neurophysiology*, *77*(4), 1906–1923.

Giesel, M., Hansen, T., & Gegenfurtner, K. R. (2009). The discrimination of chromatic textures. *Journal of Vision, 9*(9):11, 1–28, http://www.journalofvision.org/content/9/9/11, doi:10.1167/9.9.11. [PubMed] [Article]

Giulianini, F., & Eskew, R. T. (1998). Chromatic masking in the (ΔL/L, ΔM/M) plane of cone contrast space reveals only two detection mechanisms. *Vision Research*, *38*(24), 3913–3926.

Giulianini, F., & Eskew, R. T. (2007). Theory of chromatic noise masking applied to testing linearity of S-cone detection mechanisms. *Journal of the Optical Society of America (A)*, *24*(9), 2604–2621.

Goda, N., & Fujii, M. (2001). Sensitivity to modulation of color distribution in multicolored textures. *Vision Research*, *41*(19), 2475–2485.

Graham, N. V. S. (1989). *Visual pattern analyzers*. New York: Oxford University Press.

Hansen, T., & Gegenfurtner, K. R. (2006). Higher level chromatic mechanisms for image segmentation. *Journal of Vision, 6*(3):5, 239–259, http://www.journalofvision.org/content/6/3/5, doi:10.1167/6.3.5. [PubMed] [Article]

Hansen, T., Giesel, M., & Gegenfurtner, K. R. (2008). Chromatic discrimination of natural objects. *Journal of Vision, 8*(1):2, 1–19, http://www.journalofvision.org/content/8/1/2, doi:10.1167/8.1.2. [PubMed] [Article]

Irtel, H. (1992). Computing data for color-vision modeling. *Behavior Research Methods, Instruments, & Computers, 24,* 397–401.

Judd, D. B. (1951). Report of U.S. secretariat committee on colorimetry and artificial daylight. *Proceedings of the Twelfth Session of the CIE*. (p. 11). Paris: Bureau Central de la CIE.

Kiper, D. C., Fenstemaker, S. B., & Gegenfurtner, K. R. (1997). Chromatic properties of neurons in macaque area V2. *Visual Neuroscience*, *14*(6), 1061–1072.

Knoblauch, K. (1995). Dual bases in dichromatic color space. In B. Drum (Ed.), *Color vision deficiencies* (Vol. XII, pp. 165–177). Dordrecht: Kluwer.

Knoblauch, K., & D'Zmura, M. (2001). Reply to letter to editor by M. J. Sankeralli and K. T. Mullen published in *Vision Research, 41,* 53–55: Lights and neural responses do not depend on choice of color space. *Vision Research*, *41*(13), 1683–1684.

Komatsu, H. (1998). Mechanisms of central color vision. *Current Opinion in Neurobiology*, *8*(4), 503–508.

Komatsu, H., Ideura, Y., Kaji, S., & Yamane, S. (1992). Color selectivity of neurons in the inferior temporal cortex of the awake macaque monkey. *Journal of Neuroscience*, *12*(2), 408–424.

Krantz, D. H. (1975). Color measurement and color theory: I. Representation theorem for Grasmann structures. *Journal of Mathematical Psychology, 12,* 283–303.

Krauskopf, J. (1999). High order color mechanisms. In K. R. Gegenfurtner & L. T. Sharpe (Eds.), *Color vision: from genes to perception* (pp. 303–317). New York: Cambridge University Press.

Krauskopf, J., & Gegenfurtner, K. (1992). Color discrimination and adaptation. *Vision Research*, *32*(11), 2165–2175.

Krauskopf, J., Williams, D. R., & Heeley, D. W. (1982). Cardinal directions of color space. *Vision Research, 22,* 1123–1131. [PubMed]

Krauskopf, J., Williams, D. R., Mandler, M. B., &

Brown, A. M. (1986). Higher order color mechanisms. *Vision Research*, 26(1), 23–32. [PubMed]

Legge, G. E., Kersten, D., & Burgess, A. E. (1987). Contrast discrimination in noise. *Journal of the Optical Society of America (A)*, 4(2), 391–404.

Lennie, P., Krauskopf, J., & Sclar, G. (1990). Chromatic mechanisms in striate cortex of macaque. *Journal of Neuroscience, 10*, 649–69.

Levitt, H. L. (1971). Transformed up-down method in psychophysic. *Journal of the Acoustic Society of America, 49*, 476–477.

Li, A., & Lennie, P. (1997). Mechanisms underlying segmentation of colored textures. *Vision Research*, 37(1), 83–97.

Lindsey, D. T., & Brown, A. M. (2004). Masking of grating detection in the isoluminant plane of DKL color space. *Visual Neuroscience*, 21(3), 269–273.

MacLeod, D. I., & Boynton, R. M. (1979). Chromaticity diagram showing cone excitation by stimuli of equal luminance. *Journal of the Optical Society of America*, 69(8), 1183–1186.

McGraw, P. V., McKeefry, D. J., Whitaker, D., & Vakrou, C. (2004). Positional adaptation reveals multiple chromatic mechanisms in human vision. *Journal of Vision, 4*(7):8, 626–636, http://www.journalofvision.org/content/4/7/8, doi:10.1167/4.7.8. [PubMed] [Article]

McKeefry, D. J., McGraw, P. V., Vakrou, C., & Whitaker, D. (2004). Chromatic adaptation, perceived location, and color tuning properties. *Visual Neuroscience*, 21(3), 275–282.

Pelli, D. (1981). *The effect of visual noise*. Unpublished doctoral thesis, Cambridge University, Cambridge, United Kingdom.

Sankeralli, M. J., & Mullen, K. T. (1997). Postreceptoral chromatic detection mechanisms revealed by noise masking in three-dimensional cone contrast space. *Journal of the Optical Society of America (A)*, 14(10), 2633–2646.

Sankeralli, M. J., & Mullen, K. T. (2001). Assumptions concerning orthogonality in threshold scaled versus cone-contrast colour spaces. *Vision Research*, 41(1), 53–55.

Smith, V. C., & Pokorny, J. (1975). Spectral sensitivity of the foveal cone photopigments between 400 and 500 nm. *Vision Research*, 15(2), 161–171.

Stevens, S. S., Yantis, S., & Pashler, H. (Eds.). (2004). *Stevens' handbook of experimental psychology* (Vol. 1, 3rd ed.). New York: John Wiley and Sons.

Stockman, A., & Brainard, D. H. (2009). Color vision mechanisms. In M. Bass (Ed.), *OSA handbook of optics: Vol. III. Vision and vision optics* (3rd ed., pp. 11.1–11.104). New York: McGraw-Hill.

Stockman, A., & Sharpe, L. T. (1999). Cone spectral sensitivities and color matching. In K. R. Gegenfurtner & L. T. Sharpe (eds.), *Color vision—From genes to perception* (pp. 3–51). New York: Cambridge University Press.

Stockman, A., & Sharpe, L. T. (2000). The spectral sensitivities of the middle- and longwavelength-sensitive cones derived from measurements in observers of known genotype. *Vision Research*, 40(13), 1711–1737.

Stockmann, A. (2007). Colour & vision research laboratory and database. http://www.cvrl.org/ (Accessed May 25, 2007).

Stromeyer, C. F., Thabet, R., Chaparro, A., & Kronauer, R. E. (1999). Spatial masking does not reveal mechanisms selective to combined luminance and red-green color. *Vision Research*, 39(12), 2099–2112.

Wachtler, T., Sejnowski, T. J., & Albright, T. D. (2003). Representation of color stimuli in awake macaque primary visual cortex. *Neuron*, 37(4), 681–691.

Watson, A. B., & Robson, J. G. (1981). Discrimination at threshold: labeled detectors in human vision. *Vision Research*, 21(7), 1115–1122.

Webster, M. A., & Mollon, J. D. (1991). Changes in colour appearance following post-receptoral adaptation. *Nature*, 349(6306), 235–238.

Wyszecki, G., & Stiles, W. S. (1982). *Color science. Concepts and methods, quantitative data and formulae* (2nd ed.). New York: Wiley.

Zaidi, Q., & Halevy, D. (1993). Visual mechanisms that signal the direction of color changes. *Vision Research*, 33(8), 1037–1051.

Zaidi, Q., & Shapiro, A. G. (1993). Adaptive orthogonalization of opponent-color signals. *Biological Cybernetics*, 69(5–6), 415–428.

Appendix A: Notations

In the present article we deal with two *color spaces* that are used to define light modulations (CC and DKL space) and two corresponding *mechanism spaces* that are dual to the color spaces (the space of cone mechanisms and second-stage mechanisms). Since there is no standardized notation, a summary of our notation may be helpful for some readers.

Cone mechanisms

S, M, L

Cone contrast space

S/ΔS, M/ΔM, L/ΔL Axes of cone contrast space

ΔL/ΔM   The plane in CC space spanned by the axes L/ΔL and M/ΔM

ΔS/ΔL   The plane in CC space spanned by the axes S/ΔS and L/ΔL

ΔS/ΔM   The plane in CC space spanned by the axes S/ΔS and M/ΔM

Second-stage mechanisms (also called cardinal, DKL, or postreceptoral mechanisms)

L + M, −L − M   Achromatic mechanisms

S − (L + M), −S + (L + M)   Chromatic, S vs. (L and M) cone-opponent mechanisms

L − M, M − L   Chromatic, L vs. M cone-opponent mechanisms

Cardinal directions of color space (DKL color space)

The DKL color space can be defined based on the second-stage mechanisms. A light modulation along a cardinal direction silences two pairs of second-stage mechanism. A cardinal direction is a line passing through the origin (0, 0, 0) that is orthogonal to the plane spanned by two second-stage mechanisms.

L/M/S   Cardinal achromatic direction
Colors vary from black to white
Orthogonal to the chromatic mechanisms and sensed only by the pair of achromatic mechanisms

S   Cardinal chromatic direction
Colors vary from lime to violet
Orthogonal to the mechanisms in the ΔL/ΔM plane
Only the response of S cones vary, L and M cone responses remain constant
Tritanopic confusion line: colors along this line cannot be discriminated by a tritanop, i.e., an observer without S cones

L/M   Cardinal chromatic direction
Colors vary from teal to cherry
Orthogonal to the pair of achromatic mechanism and to the pair of S vs. (L and M) cone-opponent mechanisms
Only the responses of L and M cones vary at a constant sum, S cone responses remain constant

Appendix B: Definition of the DKL color space

To define the a DKL color space one has to

• Specify the axes of the color space with respect to a standardized color space. There are two different methods to define the axes, which are formally equivalent (Knoblauch, 1995):

a. Based on the cardinal directions, i.e., in terms of the stimuli that isolate the second-stage mechanisms (Zaidi & Halevy, 1993). This is the typical approach.

b. Based on the second-stage mechanisms, i.e., in terms of the response properties of the mechanisms (Brainard, 1996). This approach is atypical but has the advantage that it is explicitly based on the model underling the DKL color space.

• Define the scaling of the axes. There are two different methods to scale the axes:

a. Device dependent: Setting the maximum excursion along each axis that falls within the gamut of the display used to unity. This method is simple because no further measurements or data are needed, but it has the disadvantage that it depends on the properties of the display device.

b. Observer dependent: By setting the average detection threshold of a number of observers along each axis to unity. This method is more complex because detection thresholds need to be measured and has the disadvantage that is depends on the average performance of the chosen observers.

Both scaling methods are likely to vary between studies, and consequently the scaling of the axes varies across studies. The scaling of the axis is important because it defines the color of intermediate angles. "There is no official standardization of DKL color space, and thus no accepted specification of color angles other than the L_o/M_o and S_o axes" (De Valois, De Valois, & Mahon, 2000, p. 512). Fortunately, the variations within each scaling method are small if the gamut of different CRTs or the average thresholds of different observers are similar, as is usually the case. For example, De Valois et al. (2000, p. 512) reported "Along the L_o/M_o axis, the L and M cone contrasts were 8% and 16%, respectively, and along the S_o axis, the S cone contrast was 83%." The corresponding values in the present study are 7.63%, 14.35%, and 80.61% of L, M, and S cone contrasts.

Note that DKL is a contrast space, i.e., the origin (0, 0, 0) of DKL space is the white point of the monitor used to present the stimuli. Therefore, absolute chromaticity coordinates, e.g., in CIE xyY space differ between studies.

We used the procedure outlined in Zaidi and Halevy (1993). We define the axes of the DKL color space by specifying the cardinal directions with respect to the Judd correction of the CIE 1931 color space and use a device-dependent scaling of the axes. We shall outline the procedure to define the DKL color space by computing the conversion matrix from RGB to DKL. This can be done in the following three steps:

1. Measure the monitor spectra of the three primaries RGB at maximum intensity, i.e., with RGB values (255, 0, 0), (0, 255, 0), and (0, 0, 255). We measured these values under conditions similar to the experiment. Therefore, we presented colored squares on a light gray background. The size of the square matched the size of the stimulus used in the experiment. The RGB values of the light gray background were (192, 192, 192) to approximate the estimated RGB values of the white point of neutral gray (0.5, 0.5, 0.5) after gamma correction ($192 \approx 255\,[0.5^{\{1/\gamma\}}]$) for an assumed gamma value of $\gamma = 2.4$). We used a Photo Research PR-650 spectroradiometer (Photo Research, Chatsworth, CA) to measure the spectra.
2. Compute the S, M, L cone excitation of the monitor spectra.

Let Φ be a spectra matrix whose columns are given by the monitor spectra, and let $\bar{C} = (\bar{l}\ \bar{m}\ \bar{s})$ be a matrix of spectral sensitivities whose columns are given by a set of cone fundamentals (sampled at the wavelengths corresponding to the monitor spectra). Then the response matrix C of the cones is given by

$$C = \bar{C}\Phi$$

3. Determine the coefficients of the conversion matrix from RGB to DKL.

First we consider the L/M axis that is defined by two properties:

a. The excitations of S cones do not change along the L/M axis. Since all cardinal directions intersect at the white point, any color $\mathbf{x} = (r_x, g_x, b_x)^T$ along the L/M axis has the same S cone excitation as the white point $\mathbf{w} = (r_w, g_w, b_w)^T$:

$$\mathbf{s}^T\mathbf{x} = \mathbf{s}^T\mathbf{w}$$

b. L and M cones vary at a constant sum along the L/M axis. Therefore, the sum of the L and M cone excitation at any point along the L/M axis is the same as the sum he sum of the L and M cone excitation at the white point $\mathbf{w}$:

$$(\mathbf{m} + \mathbf{l})^T\mathbf{x} = (\mathbf{m} + \mathbf{l})^T\mathbf{w}.$$

The only unknown in the two equations is $\mathbf{x} = (r_x, g_x, b_x)^T$. The RGB values for the full gamut of displayable colors along the L/M axis are found be simultaneously solving the two equations as r_x varies from 0 to 1.

Solving for g_x results in

$$g_x = r_w \frac{s_R L_B / s_B - L_R}{s_G L / s_B - L_G}.$$

Solving for b_x results in

$$b_x = r_w \frac{s_R L_G / s_G - L_R}{s_B L_G / s_G - L_B}.$$

To shorten the equation we have defined $L_X = m_X + l_X$ as the sum of the M and L cone responses to a monitor primary $X \in \{R, G, B\}$.

Second we consider the S axis in the same way. Along the S axis only the S cone excitation changes such that for any color $\mathbf{y} = (r_y, g_y, b_y)^T$ along the S axis the responses of the L and M cones are the same at the white point:

$$\mathbf{m}^T\mathbf{y} = \mathbf{s}^T\mathbf{w} \quad \text{and} \quad \mathbf{l}^T\mathbf{y} = \mathbf{s}^T\mathbf{w}.$$

The RGB values for the full gamut of displayable colors the along the S axis are found by simultaneously solving the two equations as b_y varies from 0 to 1.

Solving for g_y results in

$$g_y = b_w \frac{s_B Q_G - m_B}{l_R Q_G - m_R}.$$

Solving for r_y results in

$$r_y = b_w \frac{s_B Q_R - m_B}{l_R Q_R - m_R}.$$

To shorten the equation we have defined $Q_R = m_R / l_R$ as the ratio of the M and L cone responses to the monitor primary R.

The final conversion matrix is then given by

$$\begin{pmatrix} L/M/S \\ L/M \\ S \end{pmatrix} = \begin{pmatrix} 1 & 1 & r_y/r_w \\ 1 & -g_x/g_w & -g_y/g_w \\ 1 & -b_x/b_w & -1 \end{pmatrix} \begin{pmatrix} R \\ G \\ B \end{pmatrix}.$$